Department of Energy
Office of Civilian Radioactive Waste Management
Yucca Mountain Site Characterization Office
P.O. Box 364629
North Las Vegas, NV 89036-8629

QA: N/A

JUN 27 2002

OVERNIGHT MAIL

Janet R. Schlueter, Chief
High-Level Waste Branch
Division of Waste Management
Office of Nuclear Materials Safety
and Safeguards
U.S. Nuclear Regulatory Commission
Two White Flint North
Rockville, MD 20852

TRANSMITTAL OF INFORMATION ADDRESSING KEY TECHNICAL ISSUE (KTI) AGREEMENT ITEMS RADIONUCLIDE TRANSPORT (RT) 3.06 AND STRUCTURAL DEFORMATION AND SEISMICITY (SDS) 3.02

References: (1) Ltr, Brocoum to Reamer, dtd 3/12/01
(2) Ltr, Reamer to Brocoum, dtd 2/6/02

RT 3.06 and SDS 3.02 are identical KTI agreements in which the U.S. Department of Energy (DOE) agreed to provide the pre-test predictions for Alcove 8 – Niche 3 work. In response to these agreements, DOE transmitted by Reference 1 the document entitled *Pre-Test Predictions for Alcove 8 – Niche 3 Crossover Test* (Pre-Test Prediction Report).

Reference 2 provided the results of the U.S. Nuclear Regulatory Commission review of the Pre-Test Prediction Report, and identified three additional information needs:

1. Provide the pre-test predictions for the Phase II test components;

2. Provide clarification of whether the tracer transport results for the small plot tests discussed in the Pre-Test Prediction Report, and the pre-test predictions in Attachment II to the Pre-Test Prediction Report, are the pre-test predictions for the Small Plot Test or the Line Release (Fault) Test, or both; and

3. Provide clarification on the specific test objectives of the Line Release (Fault) Test.

YMP-5

The following is provided in response to the information needs:

1. Planning for the Phase II pre-test predictions is currently being finalized. These predictions will be available after fiscal year 2002.

2. The tracer transport results for the small plot tests discussed in the Pre-Test Prediction Report, and the pre-test predictions in Attachment II to the Pre-Test Prediction Report, are the pre-test predictions for the Small Plot Test.

3. As stated in the enclosure, "The main objectives of the Line Release (Fault) Test include quantification of large-scale (~20 m) infiltration and seepage processes in the potential repository horizon, estimation of relations between relative permeability and water potential for unsaturated flow in faults and fracture networks, and evaluation of the importance of matrix diffusion in unsaturated zone (UZ) transport processes."

This letter also transmits the report *Updated Pre-Test Predictions of Tracer Transport for Alcove 8 – Niche 3 Cross-Over Fault (Phase 1)*, which includes the pre-test predictions for the Cross-Over Fault Test (also called the Linear Release Test) (Phase 1).

DOE considers the information provided above and in the enclosure to fulfill RT 3.06 and SDS 3.02 and the associated additional information needs, except for the pre-test predictions for Phase II test which are not yet available. Additionally, since these two agreements are identical, DOE suggests that SDS 3.02 could be closed, and the remaining information need tracked by RT 3.06.

This letter contains no new regulatory commitments. Please direct any questions concerning this letter and its enclosure to Timothy C. Gunter at (702) 794-1343 or Eric T. Smistad at (702) 794-5073.

Joseph D. Ziegler
Acting Assistant Manager, Office of
Licensing and Regulatory Compliance

OL&RC:TCG-1316

Enclosure:
Updated Pre-Test Predictions of Tracer Transport for Alcove 8-Niche 3 Cross-Over Fault Test (Phase I)

cc w/encl:
J. W. Andersen, NRC, Rockville, MD
D. D. Chamberlain, NRC, Arlington, TX
R. M. Latta, NRC, Las Vegas, NV
S. H. Hanauer, DOE/HQ (RW-2), Las Vegas, NV
B. J. Garrick, ACNW, Rockville, MD

cc w/encl: (continued)
Richard Major, ACNW, Rockville, MD
W. D. Barnard, NWTRB, Arlington, VA
Budhi Sagar, CNWRA, San Antonio, TX
W. C. Patrick, CNWRA, San Antonio, TX
Steve Kraft, NEI, Washington, DC
J. H. Kessler, EPRI, Palo Alto, CA
J. R. Egan, Egan & Associates, McLean, VA
Alan Kalt, Churchill County, Fallon, NV
Irene Navis, Clark County, Las Vegas, NV
R. R. Loux, State of Nevada, Carson City, NV
John Meder, State of Nevada, Carson City, NV
George McCorkell, Esmeralda County, Goldfield, NV
Leonard Fiorenzi, Eureka County, Eureka, NV
Andrew Remus, Inyo County, Independence, CA
Michael King, Inyo County, Edmonds, WA
Mickey Yarbro, Lander County, Battle Mountain, NV
Lola Stark, Lincoln County, Caliente, NV
L. W. Bradshaw, Nye County, Pahrump, NV
David Chavez, Nye County, Tonopah, NV
Josie Larson, White Pine County, Ely, NV
Arlo Funk, Mineral County, Hawthorne, NV
R. I. Holden, National Congress of American Indians, Washington, DC
Allen Ambler, Nevada Indian Environmental Coalition, Fallon, NV
CMS Coordinator, BSC, Las Vegas, NV

cc w/o encl:
C. W. Reamer, NRC, Rockville, MD
N. K. Stablein, NRC, Rockville, MD
L. L. Campbell, NRC, Rockville, MD
S. L. Wastler, NRC, Rockville, MD
Margaret Chu, DOE/HQ (RW-1) FORS
A. B. Brownstein, DOE/HQ (RW-52) FORS
R. A. Milner, DOE/HQ (RW-2) FORS
S. E. Gomberg, DOE/HQ (RW-2) FORS
N. H. Slater-Thompson, DOE/HQ (RW-52) FORS
R. B. Murthy, DOE/OQA (RW-3), Las Vegas, NV
N. H. Williams, BSC, Las Vegas, NV
S. J. Cereghino, BSC, Las Vegas, NV
Donald Beckman, BSC, Las Vegas, NV
E. P. Opelski, NQS, Las Vegas, NV
K. M. Cline, MTS, Las Vegas, NV
R. B. Bradbury, MTS, Las Vegas, NV
R. P. Gamble, MTS, Las Vegas, NV
R. C. Murray, MTS, Las Vegas, NV
R. D. Rogers, MTS, Las Vegas, NV

cc w/o encl: (continued)
Richard Goffi, BAH, Washington, DC
J. R. Dyer, DOE/YMSCO, Las Vegas, NV
D. G. Horton, DOE/YMSCO, Las Vegas, NV
G. W. Hellstrom, DOE/YMSCO, Las Vegas, NV
S. P. Mellington, DOE/YMSCO, Las Vegas, NV
R. E. Spence, DOE/YMSCO, Las Vegas, NV
J. D. Ziegler, DOE/YMSCO, Las Vegas, NV
W. J. Boyle, DOE/YMSCO, Las Vegas, NV
C. M. Newbury, DOE/YMSCO, Las Vegas, NV
C. L. Hanlon, DOE/YMSCO, Las Vegas, NV
M. C. Tynan, DOE/YMSCO, Las Vegas, NV
T. C. Gunter, DOE/YMSCO, Las Vegas, NV
E. T. Smistad, DOE/YMSCO, Las Vegas, NV
J. T. Sullivan, DOE/YMSCO, Las Vegas, NV
G. L. Smith, DOE/YMSCO, Las Vegas, NV
C. A. Kouts, DOE/YMSCO (RW-2) FORS
R. N. Wells, DOE/YMSCO (RW-60) Las Vegas, NV
OL&RC Library
Records Processing Center = "25"
(ENCL = READILY AVAILABLE)

Bechtel SAIC Company, LLC

Updated Pre-Test Prediction of Tracer Transport for Alcove 8-Niche 3 Cross-Over Fault Test (Phase I)

June 2002

Prepared by:

H. H. Liu — 6-19-02 Date

Approved by:

Joe Wang
UZ Department Manager — 6/20/02 Date

ENCLOSURE

Updated Pre-Test Prediction of Tracer Transport for Alcove 8-Niche 3 Cross-Over Fault Test (Phase I)

1. Introduction

Infiltration and tracer tests are being conducted at the cross-over test site where Alcove 8 in the Enhanced Characterization of Repository Block (ECRB) Cross Drift is about 20 m directly above Niche 3 which is located in the Exploratory Studies Facility (ESF) Main Drift. The major test objectives include quantification of large-scale (~20 m) infiltration and seepage processes in the potential repository horizon, estimation of the relationships between relative permeability and water potential for unsaturated flow in faults and fracture networks, and evaluation of the importance of matrix diffusion in unsaturated zone (UZ) transport processes.

The tests consist of several phases. In each phase, liquid (with or without tracers) is released from infiltration plots at Alcove 8 and detected at Niche 3. In Phase I, a water pressure head of 2 cm will be kept at the infiltration plots, while the infiltration rate will be reduced step by step in the subsequent phases of the test. In addition to practical considerations for performing the tests, use of this test condition for Phase I allows matrix blocks near fracture-matrix interfaces within flow paths to have relatively high saturation. Because of this, matrix imbibition is considerably reduced in the later stage of Phase I and other phases of the tests. Significant matrix imbibition would make evaluating the importance of matrix diffusion difficult. The Alcove 8-Niche 3 cross-over tests are planned to be conducted at two locations in Alcove 8 using the same test procedure at each location. They correspond to small and large infiltration plots, respectively with the small plot associated with a nearly vertical fault. This report deals with modeling results for Phase I of the small-plot (fault) tests.

Preliminary modeling studies were performed to predict the small-plot test results for Phase I (Liu 2001, Attachment II). However, since then, a number of modifications of test conditions have been made for practical reasons, and some test data have been collected. The tracer test (Phase I) started on October 1, 2001. This report provides updated predictions for the tracer test by taking into consideration changes in test conditions and data from the small-plot tests.

2. Previous Prediction Results and Test Observations

Previous modeling results indicated that simulated wetting-front arrival time at Niche 3 is very sensitive to fracture permeabilities. The predicted time for seepage to occur ranges from less than one day to longer than one hundred days (Liu 2001, Figure II-2). The tracer arrival times also range from less than one day to about one hundred days (Figure 13, Liu 2001) after tracers are introduced at the infiltration plot.

The infiltration rates at the small plot have been measured by the U.S. Geological Survey (David Hudson, input request # 00464.T), and the seepage at Niche 3 has been collected by Lawrence Berkeley National Laboratory (Rohit Salve, input request # 00463.T). The observed time for seepage to occur at Niche 3 was about 37 days after water was first released in Alcove 8 (Figure 1), which is within the predicted range. However, the observed recoverability of seepage is much lower than the predicted values when seepage rate is approximately stabilized at Niche 3. The recoverability is defined as the total volume of water collected at Niche 3 divided by the total volume of water applied from the infiltration plot over a given period of time. Predicted values for the recoverability ranges approximately from 20% to 60% (Figures II-2 and II-3, Liu 2001). Observed recoverability is less than 10%, although the seepage rate observed at Niche 3 seems to stabilize after 60 days (Figure 1).

The discrepancy between predicted and observed results is believed to partially result from the following factors. First, in the modeling prediction of Liu (2001), the length of infiltration plot was assumed to be one meter, based on the initial test design. However, the actual length of infiltration plot used in the test is about 5 meters (to increase total

infiltration rate). Therefore, the top boundary condition used in the modeling predictions of Liu (2001) is not consistent with actual experimental conditions. Second, it was also assumed that there would be no connection between the fault and surrounding fracture networks in the modeling prediction (Liu, 2001). However, wetting features were observed from ceilings of both the main drift and Niche 3 within several meters near the fault. Therefore, it is very likely that considerable "communication" between the fault and the fracture networks exists. Third, although a constant capillary pressure head of 2 cm was kept at the infiltration plot, a substantial temporal fluctuation of infiltration rate was observed until about 66 days (Figure 2). Liu (2001) could not simulate this behavior. For a given capillary pressure, the simulated infiltration rates always reach a nearly constant (stabilized) value in a short time (Figure 2), which is also consistent with experimental observations from the trench tests performed in the UZ (David Hudson, input request #00404.T). The reason for the observed fluctuation from the test site is not totally clear at this point and will be further investigated. All these factors will be considered in the updated model to be discussed later on in this report.

Note that Br concentration in seeping water was also analyzed as a function of time by Lawrence Berkeley National Laboratory (Max Hu, DTN: LB0109NICH3TRC.001), as shown in Figure 3. The Br concentration was initially low (about 3 ppm), then increased gradually with time, reaching the value of about 30 ppm (that is the same as that for water applied at the infiltration plot) about 30 days after seepage occurred at Niche 3. This may indicate the importance of matrix diffusion, evaluation of which is an important objective of the tests. If there is no matrix diffusion at all, the Br concentration should be a constant (30 ppm) with time. In addition to matrix diffusion, other mechanisms (such as sorption) may also contribute to the observed retardation of Br transport. However, Br is generally considered conservative, and the potential sorption is expected to play a minor role in the observed retardation. Considering that Br concentration data are available only for one of many trays used for collecting seepage at Niche 3 and it is computationally extensive to simulate tracer transport for the given test conditions, the Br data were not used for model calibration in this study.

3. Updated Model and Model Calibrations

3.1. Modeling approaches

As previously discussed, there may be considerable communication between the fault and the surrounding fracture networks. To investigate this possibility, in this study we develop two models with the same model domain. The first model considers connections between fracture networks, while the second one completely ignores the effects of fracture networks. The second model is essentially the same as that discussed in Liu (2001). The actual communication between the fault and the fracture networks is expected to be bounded by these two models.

The fault is treated as a two-dimensional vertical fracture. The model domain extends about 25 m in the vertical direction and about 27 m in the horizontal direction (Figure 4). It is considered to be large enough, compared with size of the niche and the infiltration application area, such that side boundaries have an insignificant effect on flow and transport near the alcove. The fine grid is used for the area around the niche, and a relatively coarse grid is used elsewhere. In the direction normal to the fault, the model domain extends 3 m on each side of the fault. (Again, a very fine grid is used near the fault in this direction.) A dual-permeability model is used to deal with interaction between fracture networks and the matrix. The ITOUGH2 code (Finsterle 1997) is employed for modeling infiltration/seepage processes, and the T2R3D code (Wu et al. 1996) for modeling the tracer transport.

A constant pressure head (2 cm) or observed infiltration rate as a function of time is imposed on the top boundary (corresponding to the infiltration plot) for model prediction and calibration, respectively, while a zero-flow condition in the vertical direction is used for the rest of the top boundary. (Ambient percolation flux is expected to be insignificant compared with the infiltration rates from the infiltration plot.) The reasons for using different top boundary conditions for model calibration and prediction are discussed in Sections 3.2 and 4 of this report. The side boundary corresponds to a zero-flow condition in the radial direction, with niche wall modeled by a zero capillary-pressure condition, representing a relative humidity of 100% in the niche. The bottom boundary condition is

approximated by a free drainage condition. Initially, matrix saturations within the model domain are assumed to be the average ones under ambient conditions (given in Table 1) (Flint 1998). A small fracture saturation of 1.05% is assumed as the initial condition for fractures. Note that seepage into Niche 3 is allowed to occur from the intersection between the fault and Niche 3 and other parts of ceilings of Niche 3 in the first model. In this study, we focused on seepage from the fault only, because seepage data have not been collected for other flow paths owing to some technical reasons. The drift-scale property set (Table 1) is employed in this modeling study (with some of these properties modified during the model calibration procedure). Because of the scale of the problem, the drift-scale properties are considered to be more suitable than the site-scale ones.

3.2. Modeling calibration with infiltration-rate data

As previously discussed, although a capillary pressure head of 2 cm has been kept at the infiltration plot, considerable temporal variation of infiltration rate has been observed. While reasons for this variation are not totally clear at this point, we focused on infiltration rate data after 56 days. During this period of time, temporal fluctuation is reduced and infiltration rate seems to be stabilized (Figure 2). An average value of 250.46 L/day for this period of time was used for model calibration.

Sensitivity studies indicated that the simulated infiltration rate for the given pressure head (2 cm) is mainly determined by the fracture permeability of the top geological unit (Tsw 33) (Figure 4). Therefore, fracture permeabilities of Tsw 33 (including the permeabilities for both the fault and fracture network for the first model) were manually adjusted until the simulated infiltration rate (at 86 day) matches the observed average value (250.46 L/day). Note that the fault is considered as a vertical fracture, with the same average properties for all fractures in the corresponding fracture network. By definition of permeability, the fault permeability (corresponding to a porosity of one in the fault) is equal to the fracture permeability divided by fracture porosity. This relationship was used for calibrating fracture permeabilities for Tsw33 using the infiltration rate data. The calibrated properties are given in Table 2.

3.3. Modeling calibration with seepage-rate data

During model calibration with seepage rate data, properties for Tsw34 were adjusted only such that matches with the average infiltration-rate value still hold. The previous modeling study (Liu 2001) indicated that the simulated seepage rate is sensitive to fracture permeability, fault van Genuchten alpha, and matrix permeability when there are no connections between the fault and fracture networks. Therefore, for the second model, these parameters are adjusted during the model calibration with seepage data. For the first model, permeabilities and van Genuchten alphas for both the fault and the fracture network within Tsw34 are varied during the calibration.

As shown in Figure 2, for a given capillary pressure, the simulated infiltration rates always reach a nearly constant (stabilized) value in a short time. Therefore, as previously discussed, observed temporal variations of infiltration rate cannot be simulated with a constant capillary pressure condition at the infiltration plot. While it is important to simulate seepage with accurate infiltration rates, we used the actual infiltration rates, rather than the constant capillary pressure head, as the top boundary condition in the model calibration based on the seepage data. Calibrated properties are given in Table 2. Note that the two models match the seepage data equally well (Figure 1).

4. Model Prediction of Tracer Breakthrough Curves

After the above model calibrations, we ran the calibrated models to the time (September 5, 2001) when the tracer test is planned to start for Phase I. The simulation runs were performed with a constant capillary pressure head of 2 cm as the top boundary condition. This is because infiltration rate is stabilized at the late stage (Figure 2). The tracers are planned to be introduced within a time interval of 5 days. After that, water without tracers continue to be applied at the infiltration plot with a capillary pressure head of 2 cm. Two tracers (Br and PFBA (pentafluorobenzoic acid) with molecular diffusion coefficient values of 2.08×10^{-9} and 7.6×10^{-10} m^2/s, respectively) will be used in the test.

The previous modeling study of the Alcove 1 test showed that the dispersion process in fractures has an insignificant effect on tracer transport behavior. On the other hand, as a

result of low water flow velocity in the matrix, the mechanical dispersion in the matrix can be ignored. Consequently, dispersivity values for the fracture and matrix continua are set to zero in the tracer transport predictions. Tortuosity values for matrix diffusion are calculated using the classic formulation of Millington and Quirk (1961). Considering that matrix water saturation is close to 100% near a fracture-matrix interface when tracers are introduced, 100% matrix saturation was assumed for calculating the tortuosity values (0.54 for Tsw33 and 0.48 for Tsw34).

Figure 5 shows breakthrough curves predicted with the two calibrated models. In the figure, zero time corresponds to the time when tracers are introduced into infiltrating water. Results from both models indicate that Br generally breaks through later than PFBA and corresponds to smaller peak concentration values, because Br has a larger molecular diffusion coefficient. Therefore, the importance of the matrix diffusion may be noticed in Phase I. It is also expected that the importance of matrix diffusion will be more noticeable in the other phases because the degree of matrix diffusion depends on the residence time of infiltrating water with tracers in the rock formation. Note that the two models provide very different breakthrough curves for each tracer, although they match the seepage data equally well. This suggests that the degree of communication between the fault and the surrounding fracture network has an important impact on breakthrough curves to be observed at Niche 3.

Some factors that may considerably affect observed breakthrough curves are not considered in our simulations. For example, both tracers are considered to be conservative in our simulations, while some sorption may occur in the tests as a result of fracture coatings. On the other hand, small fractures with trace length less than 0.3 m are not considered in the predictions for Model #1. These small fractures result in a larger fracture-matrix interface area than used in the predictions and therefore enhance the matrix diffusion. We also treat the fault as a vertical fracture, which does not consider the broken zone associated with the fault. The broken zone could create a larger degree of interaction between the fault and the rock matrix. This may enhance matrix diffusion.

These factors will be considered in future comparisons between predicted and observed breakthrough curves.

5. Summary and Conclusions

Two models have been developed for predicting the breakthrough curves to be observed at Niche 3 for the Phase I tracer test. The two models have the same computational domain, but the different degrees of communication between the fault and the surrounding fracture networks. While Model #1 assumes good communication, Model #2 considers the fault to be isolated from fracture networks. Both models are calibrated against the currently available seepage and infiltration data.

Model prediction results indicate that breakthrough times for tracers are less than 5 days at Niche 3 and the peak concentration values are observed between 10 to 15 days after the tracer test starts. Both models predict that very different breakthrough curves for the two tracers (Br and PFBA) at Niche 3 as a result of matrix diffusion. The importance of matrix diffusion is thus expected to be demonstrated in the planned Phase I tracer test. Although the two models match the seepage and infiltration data equally well, they predict very different breakthrough curves for each tracer. The actual breakthrough curves to be determined from the test will be useful for estimating the communication between the fault and the surrounding fracture network. The potential effect of factors, not considered in the modeling prediction (such as small fracture, sorption of fracture coating, and the broken zone associated with the fault), will be investigated in the future.

References

Finsterle, S. 1997, ITOUGH2 Command Reference, Version 3.1, Rep. LBNL-40041, Lawrence Berkeley National Laboratory, Berkeley, CA.

Flint, L.E. 1998, Characterization of hydrologic units using matrix properties, Yucca Mountain, Nevada, USGS Water Resources Investigation Report 97-4243.

Liu, H.H, 2001, Pre-Test Predictions for Alcove8-Niche 3 Cross-over test. Bechtel SAIC Company.

Liu, H.H., Doughty, C. and Bodvarsson, G.S., 1998, An active fracture model for unsaturated flow and transport in fractured rocks, Water Resour. Res., 34(10), 2633-2646.

Millington, R.J. and Quirk, J.M., 1961, Permeability of porous solids, Trans. Faraday Soc., 57, 1200-1207.

Wu, Y.S., Ahlers, C.F., Fraser, P., Simmons, A. and Pruess, K., 1996, Software qualification of selected TOUGH2 modules, LBNL-39490, Lawrence Berkeley National Laboratory, Berkeley, CA.

Table 1. Uncalibrated rock properties (Drift-scale properties)

Rock property	TSw33		TSw34	
	Fracture	Matrix	Fracture	Matrix
[a]Permeability (m^2)	5.5E-13	3.08E-17	2.76E-13	4.07E-18
Porosity	6.6E-3	0.154	1.E-2	0.11
Fracture spacing (m)	1.23		0.23	
Fracture aperture (m)	1.49E-3		7.39E-4	
Active fracture model parameter γ	0.41		0.41	
Van Genuchten alpha (Pa^{-1})	1.46E-3	2.13E-5	5.16E-4	3.86E-6
Van Genuchten m	0.608	0.298	0.608	0.291
Residual saturation	0.01	0.12	0.01	0.19
Initial saturation	1.05E-2	0.72	1.05E-2	0.85

[a] Fault permeability is considered to be fracture permeability divided by fracture porosity (See Section 3.1), while other fault properties are assumed to be the same as those for fractures except the active fracture model parameter (Liu et al., 1998) that is zero for the fault (The fault is viewed as a single active fracture).

Table 2. Calibrated rock properties. The rock properties that are not listed in this table were fixed during inversions, and therefore are the same as those in Table 1.

(a) Model # 1

Fault permeability (m^2) (within tsw33)	8.45E-12
Fault permeability (m^2) (within tsw34)	8.74E-12
Fracture permeability (m^2) for tsw33	5.57E-14
Fracture permeability (m^2) for tsw34	1.16E-13
Fault van Genuchten alpha (Pa^{-1}) for tsw34	9.72E-4
Fracture van Genuchten alpha (Pa^{-1}) for tsw34	7.16E-3

(b) Model # 2

Fault permeability (m^2) (within tsw33)	2.83E-11
Fault permeability (m^2) (within tsw34)	5.34E-12
Matrix permeability (m^2) for tsw34	4.18E-17
Fracture van Genuchten alpha (Pa^{-1}) for tsw34	1.92E-3

Figure 1. Comparison between observed seepage rates at Niche 3 (Salve, input request # 00463.T) and model calibration results. The unit of seepage rate is L/day.

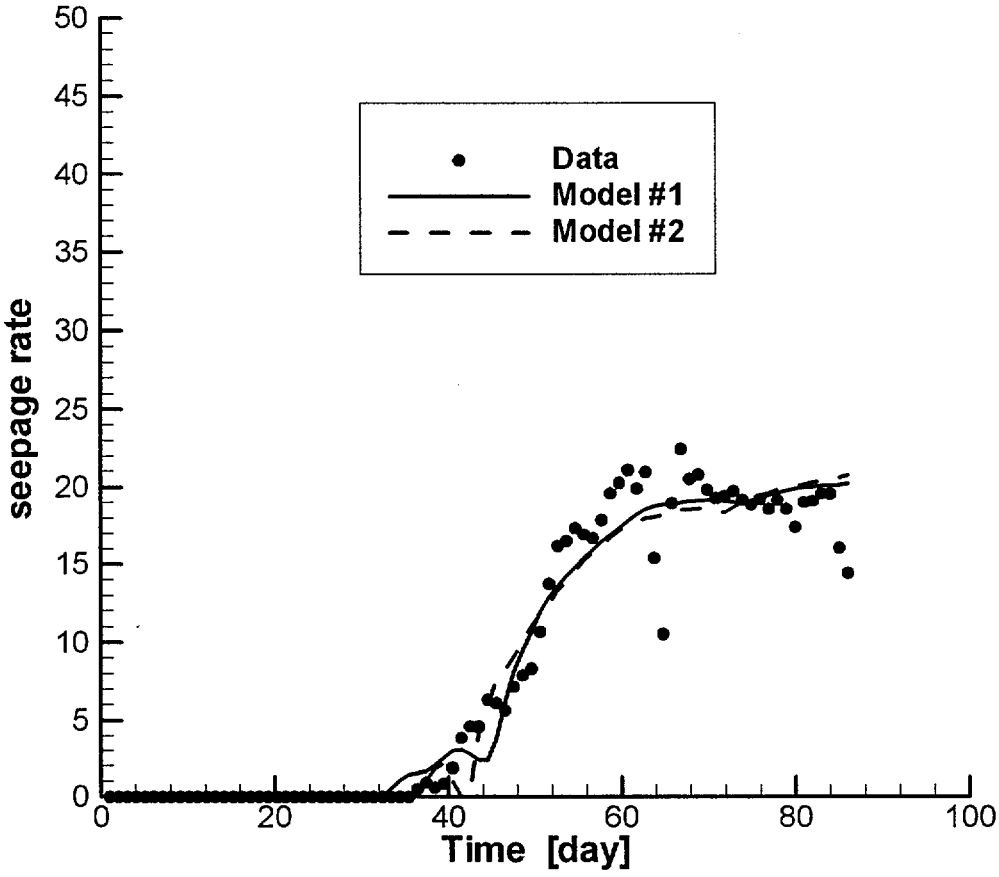

Figure 2. Comparison between observed infiltration rates at Alcove 8 (Hudson, input request # 00464.T) and model calibration results

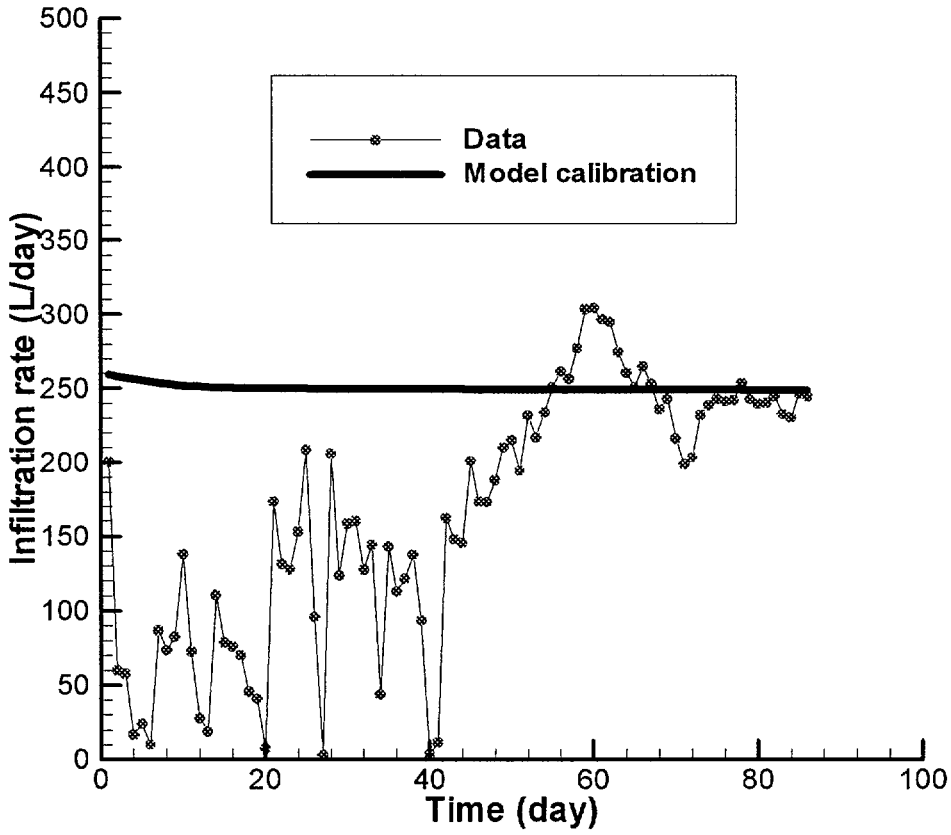

Figure 3. Measured Br concentrations for seeping water collected from tray-6 at Niche 3 (Hu, DTN:LB0109NICH3TRC.001). The solid curve represents an ideal breakthrough curve when matrix diffusion (and sorption) does not occur.

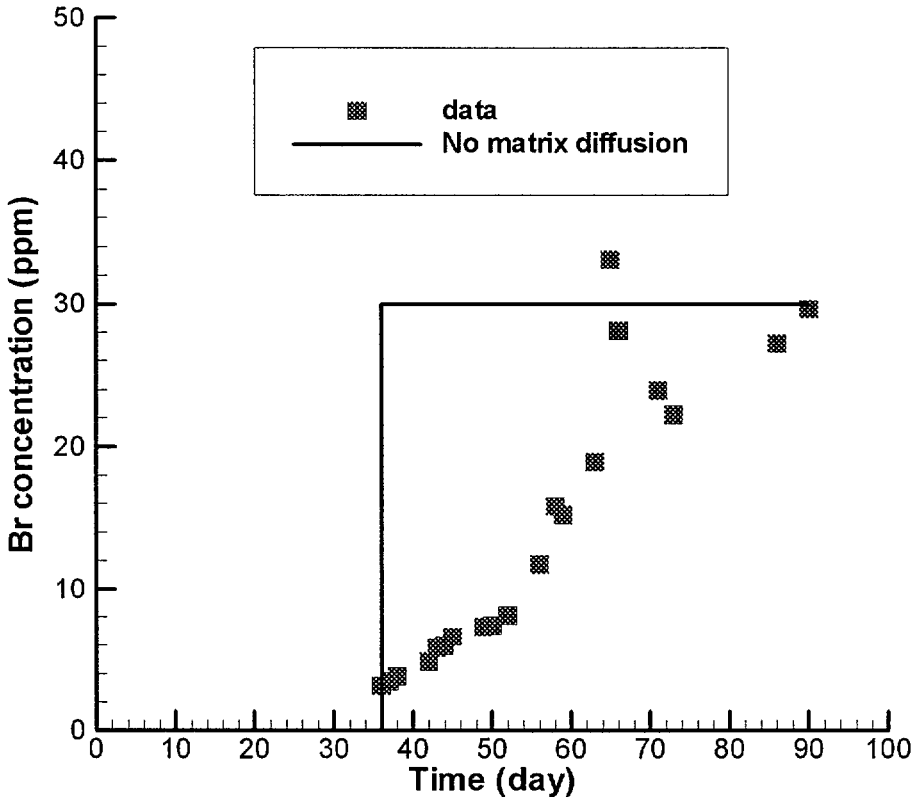

Figure 4. Numerical grid

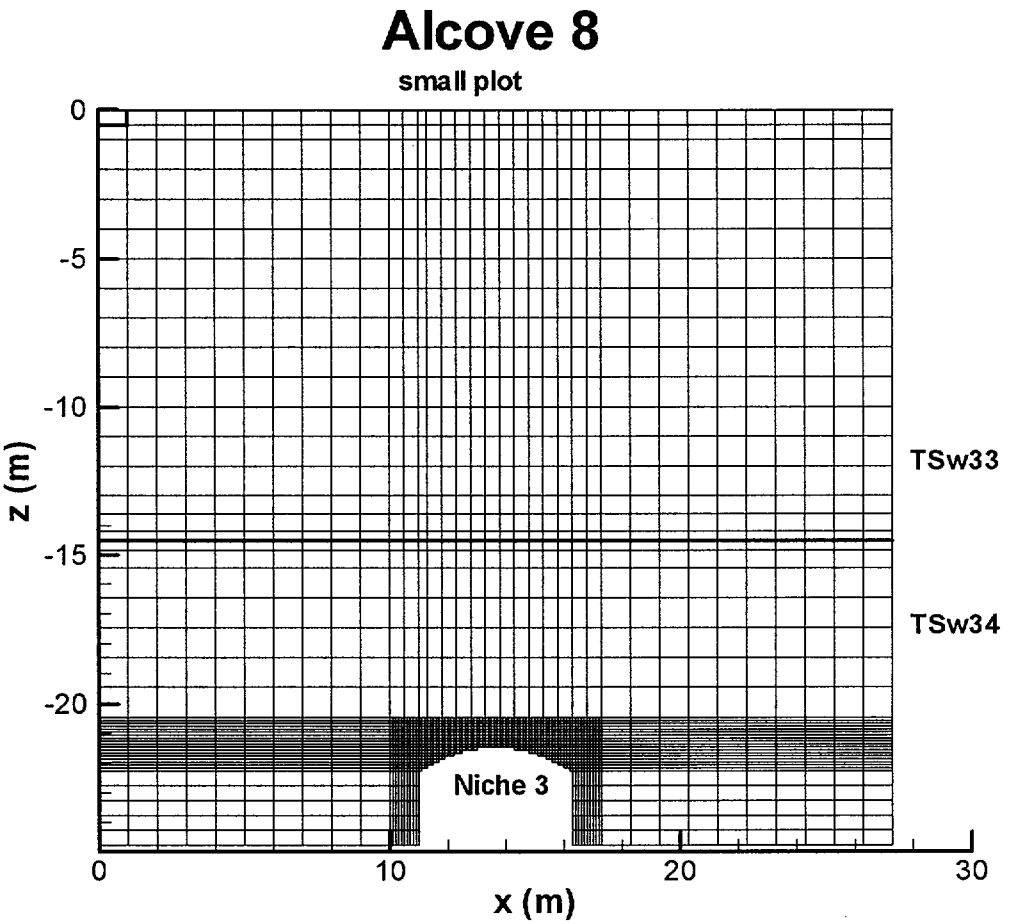

Figure 5. Predicted breakthrough curves at Niche 3 using the two calibrated models. Relative concentration refers to the average tracer concentration collected at Niche 3 divided by the tracer concentration at the infiltration plot. Time zero corresponds to the time when tracers are initially applied at the infiltration plot.

(a) Model #1

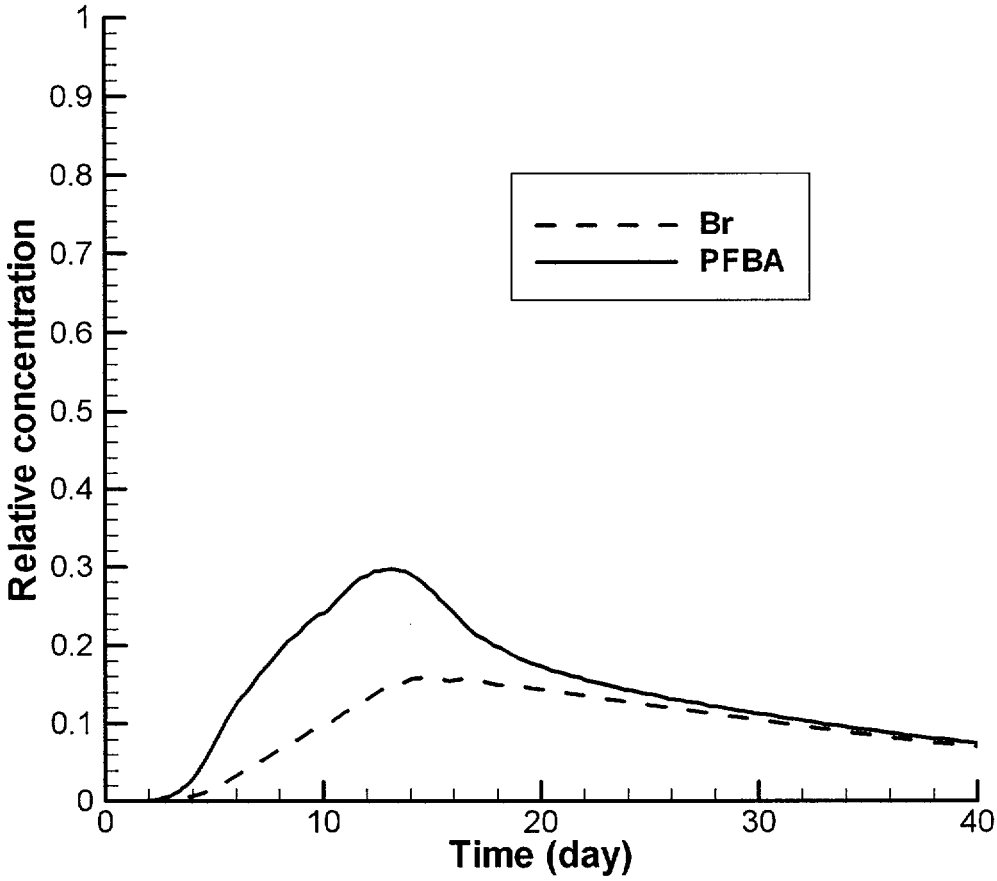

(b) Model #2

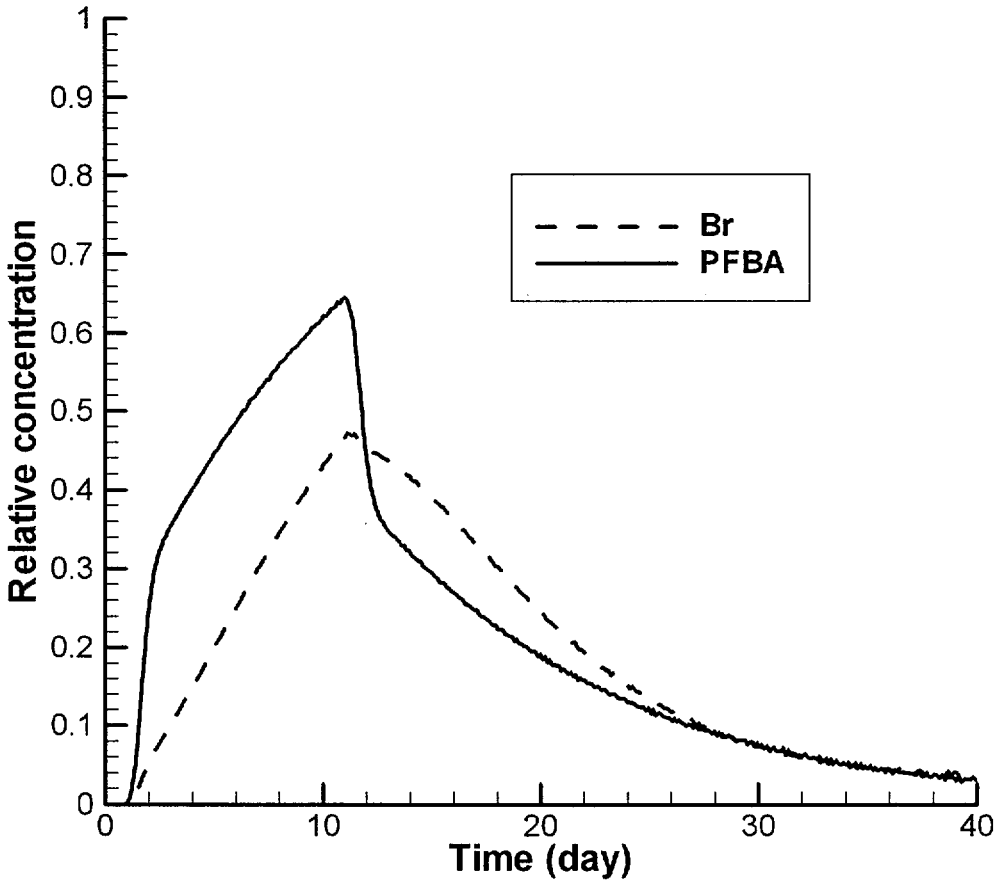
Relative concentration
Time (day)
Br
PFBA
0
0.1
0.2
0.3
0.4
0.5
0.6
0.7
0.8
0.9
1
0
10
20
30
40